Cumulative Research Findings:
NSF Grant: ATM0354545
PI: Richard Grotjahn

In this document the research findings from each year are appended and separated.

I. May 2004 – April 2005 (Year 1)
In the past 12 months (May 2004 – April 2005) we can report the following findings:

A. To see strong behaviors found in monthly mean data it was necessary to low pass filter the data; a10 days cut-off was long enough to recover correlations similar to monthly mean data but short enough to evaluate what precedes what.
B. One surprise was that stronger SLP in the Barents and GIN seas leads (not follows) a storm track shift into the Iberian Peninsula.
C. Eric deWeaver reported at the July 2004 CCSM workshop somewhat related linear calculations, his work spurred us to focus on developing a nonlinear iterative calculation in addition to the linear model calculations already planned.
D. CAM has stronger tropical connection (SLP autocorrelation) than does the NCEP/NCAR reanalysis data. See Fig. 1-1.

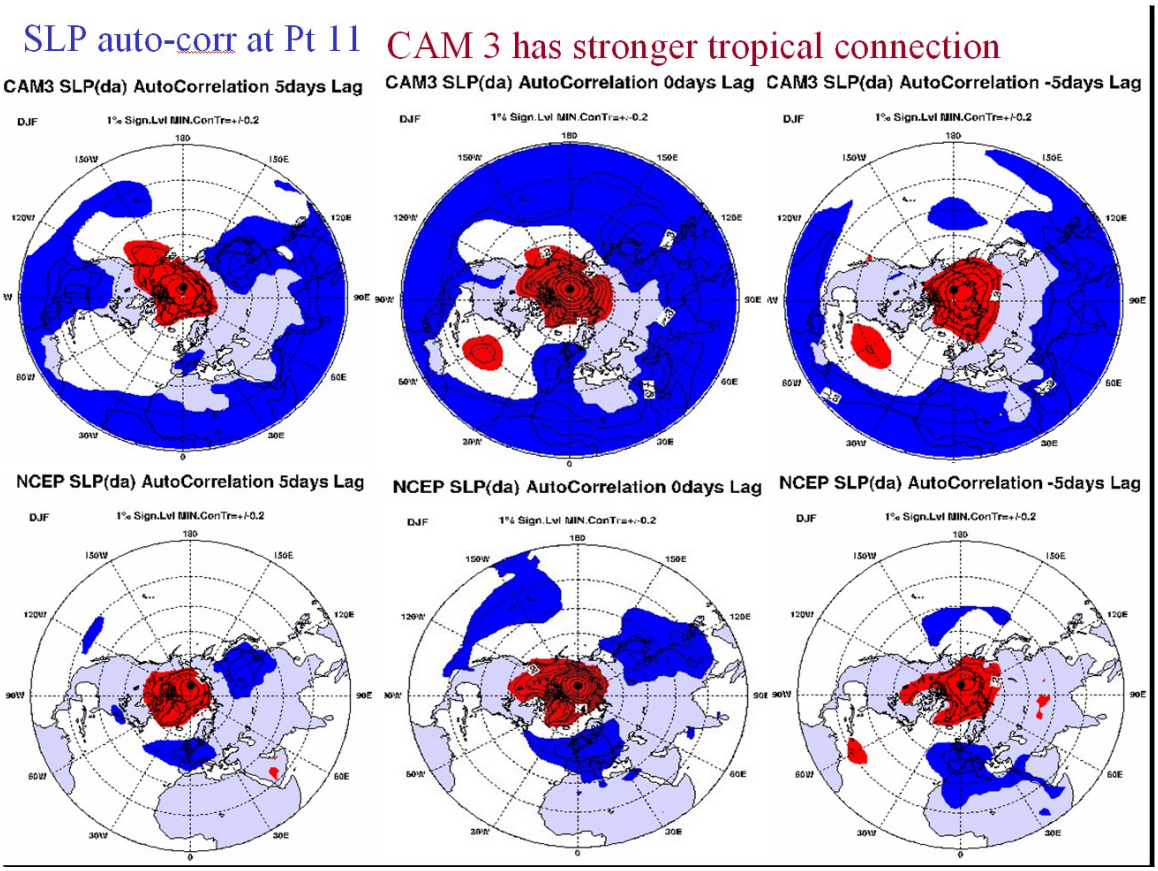

Figure 1-1. 1 point autocorrelations of CAM3 SLP and NCEP RA1 SLP for a point near center of Beaufort high (where CAM3 bias <0). The model has stronger tropical connection than observational data. Points on the Pacific side of the Beaufort high have stronger North Pacific connection in CAM3 than NCEP RA1. The figure shows a weak preference for above normal SLP over China and Mexico and below normal SLP in Alaska and adjacent Gulf to precede weaker Beaufort high. Positive correlation more easily spreads over Alaska in the model then in NCEP data, perhaps consistent with topography and surface drag hypotheses.

II. May 2005 – March 2006 (Year 2)

In the past 11 months (May 2005 – March 2006) we can report the following findings:

A. The SLP bias field has ring-like structure roughly centered near Barents Sea; to some people it looks like the AO. Since the AO is a strong internal mode of variability in the model, the AO could be stimulated by various means and therefore it would be difficult to identify primary cause(s) for the bias pattern. From CAM3 data we obtained the leading EOF of SLP (the model's form of the AO) and after interpolating to matching Gaussian grids projected that EOF onto the model SLP bias. We found that the bias was NOT like the AO. (Figure 2-1) The EOF was a small part of the bias, so internal variability cannot explain much of the bias field. Further, when the EOF was removed from the bias the resultant field looked more similar to the bias found in earlier model versions, recovering a positive maximum bias near Novaya Zemlya. This result is important because it means that it is reasonable to seek local and remote causes of the Arctic surface bias.

B. The 1-point correlation studies, did not find useful correlation with low latitude diabatic heating from precipitation (P). Both with model output and in NCEP/NCAR RA1 observations we find a significant lagged correlation with Indian Ocean P and outgoing longwave radiation (OLR). But the sense is that the Arctic SLP is occurring *before* the tropical OLR and P. Filtered daily data find correlation between high SLP near Novaya Zemlya ~5 days before P (or OLR) in the NE Indian Ocean. The correlation flips sign as the location of P (or OLR) is moved latitudinally. (Figure 2-2) The P bias field has a dipole pattern in the NW Indian Ocean consistent with the SLP bias in the Novaya Zemlya region.

C. Tests with very simple idealized heating anomalies in the SWM reproduce various parts of the SLP bias. (Figure 2-3) Cold and warm anomalies can be generated by anomalous cooling and heating forcing in the SWM. Nine such cooling/heating anomalies can match prominent cold and warm anomalies in the lower free troposphere and generate wavetrains in SWM fields, including surface pressure (our conversion to SLP is shown). Tests of the 9 anomalies singly and in combination find that anomalous cooling over Saharan and Arabian deserts has the strongest link to positive SLP near the Barents Sea maximum SLP bias. Other major cooling/heating forcing (biases) have lesser effect on the Barents region. Anomalous warming (to match a warm bias) in eastern Siberia has a prominent secondary effect on Arctic Ocean region: contributing to the Barents SLP bias max and lower SLP over the Beaufort Sea (where the model has negative bias).

D. We compared numerous large scale variables in the ERA-40 and NCEP/DOE reanalysis II datasets. The ERA-40 data seem to allow more interhemispheric transfer of information than the NCEP data. The ERA-40 data has more vigorous Hadley cells but evaporates less water in the subtropics so that both datasets have quite similar precipitation(!) The tropical Atlantic was largely missing the ICZ during DJF in NCEP data(!) However, the northern Indian Ocean seemed more reasonable in NCEP data. This study suggests that we make comparisons (and bias calculations) with ERA-40 data as well as (or in place of) NCEP data.

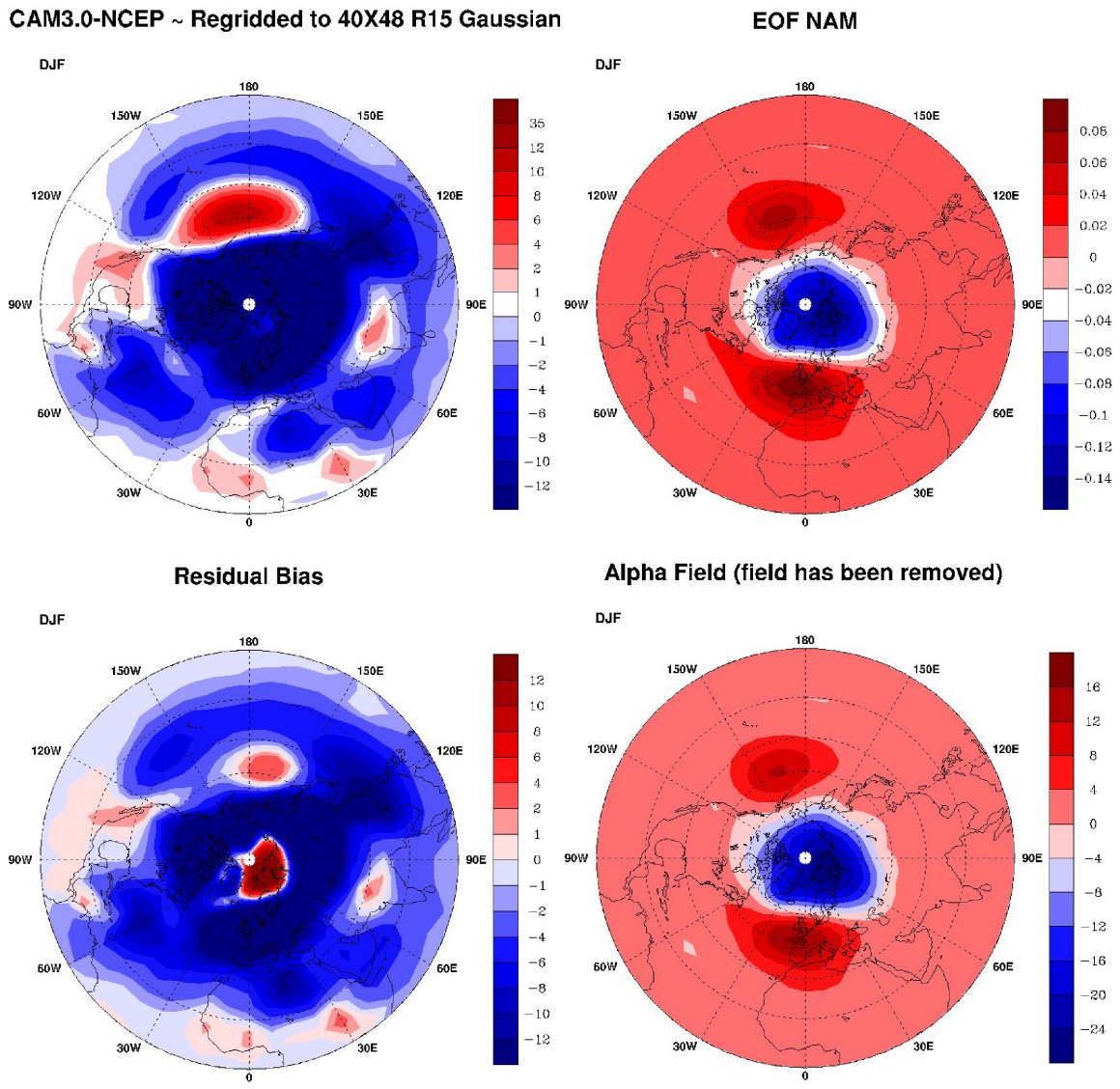

Figure 2-1. The SLP bias in CAM3 (and CCSM3) does ***not*** have a significant amount of the model's Arctic Oscillation (AO). Top left panel is CAM3 SLP bias (CAM3 minus NCEP RA I). Top right is leading EOF in CAM3, the model's form of the AO. Lower right panel is the projection of the bias onto the EOF. Lower left is the residual after removing that projection from the bias. Clearly the EOF is not a primary contributor to the SLP bias in the model. Removing the EOF produces a bias in CAM3 that more closely resembles the Arctic bias in earlier models (e.g. CCM3.6). This result is important because if the EOF was the main contributor then the SLP bias would be a natural mode of variability that could be excited by many different phenomena rather than a standing wave pattern that might be understood by distinct forcing, such as in a stationary wave model.

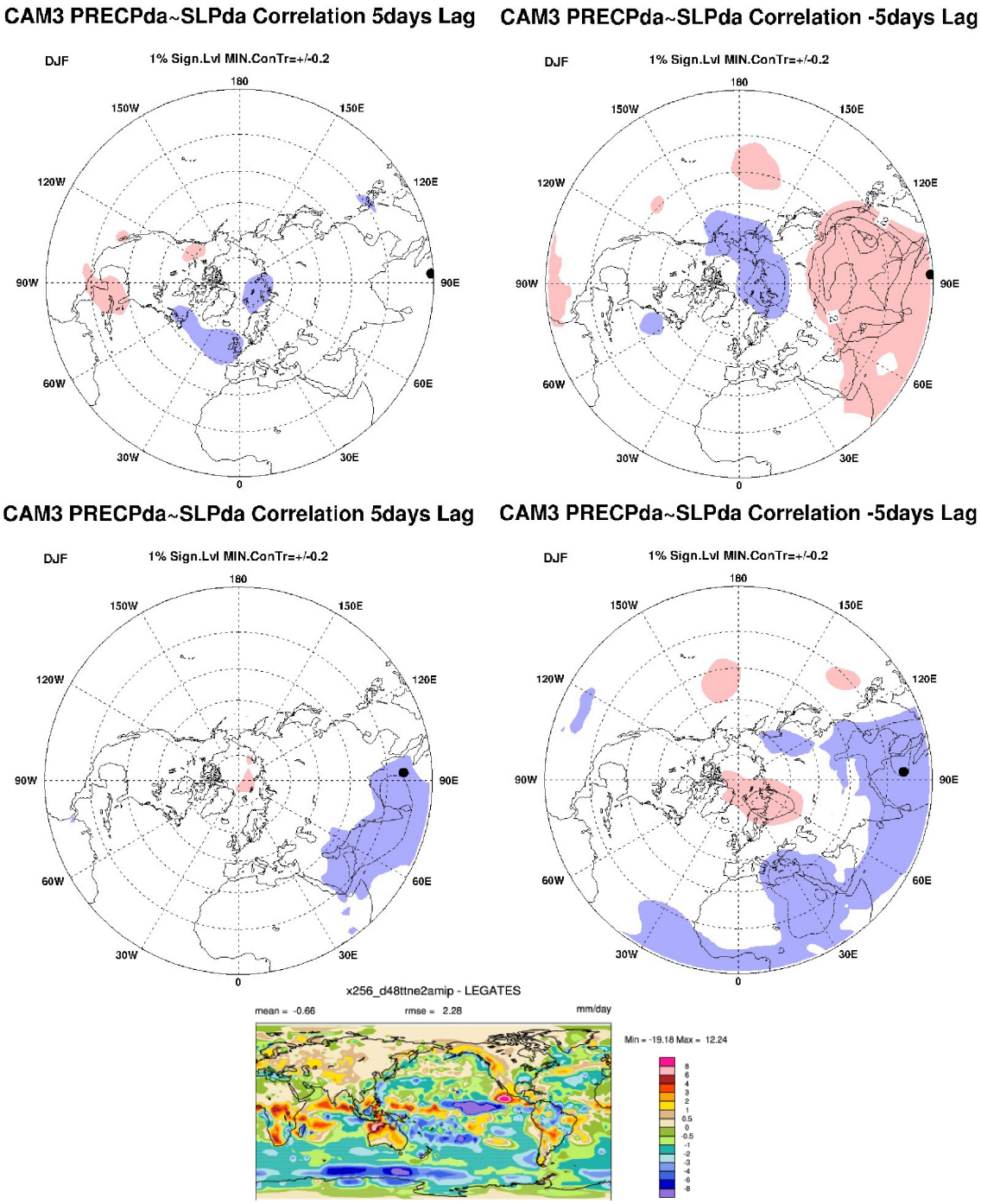

Figure 2-2. 1 point correlations of CAM3 precipitation (P at the black dot) and CAM3 SLP (2-Dimensional field). Left column, SLP correlation 5 days before value of P at black dot. Right column, SLP correlation 5 days after P at black dot. Data low pass filtered with 10d cut-off. Shaded areas pass a significance test at the 99% level. Bottom inset: CAM3 AMIP run (posted at NCAR-CGD website) which shows P bias dipole pattern in NE Indian Ocean: negative at equator (reverse sign of top row of plots) and positive at 10 N (middle row of plots). The dipoles in P bias both give SLP bias >0 near Novaya Zemlya. A similar connection is found in observed OLR and SLP.

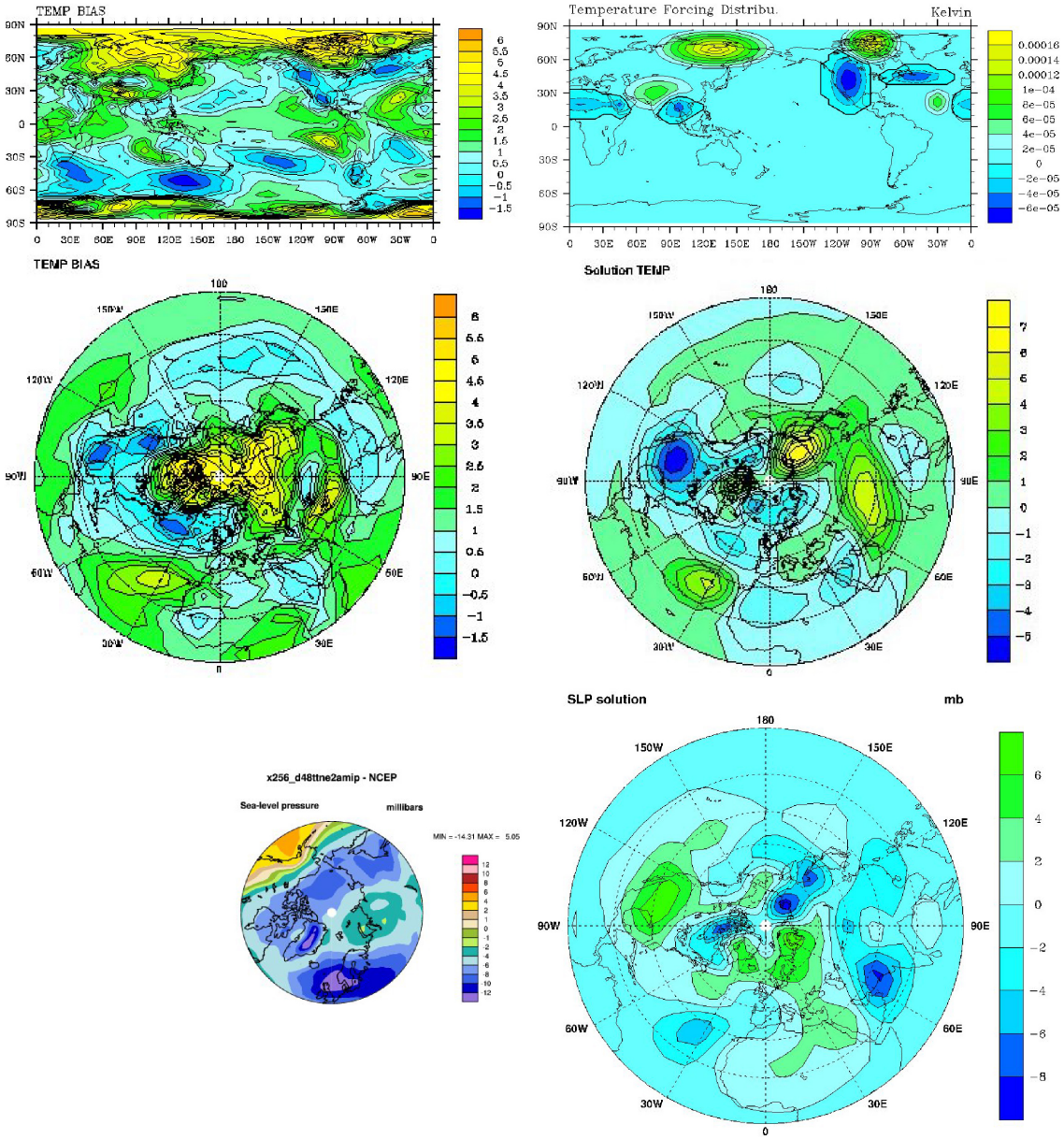

Figure 2-3. Example test calculation with anomalous T forcing in stationary wave model (SWM) of Branstator (1990) compared with bias fields. Top left, interpolated T bias at σ = 0.811 (CAM3 vs NCEP RA1, DJF); top right, 9 ellipses of T forcing input into SWM based on T bias. Middle right, SWM solution of T at σ = 0.811 for the input T forcing, Middle left, polar view of T bias for comparison. Lower right, SWM sea level pressure (SLP) solution. Lower left, SLP bias (CAM3 vs NCEP RA1, DJF; posted at NCAR-CGD website) for comparison, the small size is used so it is drawn to same scale as SWM SLP solution. The color bars vary between all panels. No tuning was done to improve the match in SLP, but extrema in T bias at 850mb guided forcing magnitudes. The key result is that the SLP bias is partly represented by a stationary wave related to T. Causes of the T forcing are diabatic and dynamic. For example, the SWM SLP max near Novaya Zemlya is most closely linked to the T forcing over the Saharan and Arabian deserts.

III. April 2006 – March 2007 (Year 3)

In the past 12 months (April 2006 – March 2007) we can report the following activities:

A. We deduced the forcing fields that create the Arctic region bias from running Branstator's SWM 'backwards'. Symbolically, the SWM can be written as: Ax = F where F is the forcing, x is the solution sought, and A is a very large square matrix dependent on the basic state (3-dimensional DJF fields of vorticity, divergence, temperature, and ln of surface pressure). To run the SWM 'backwards' we specify x and find the F. By specifying the bias fields as x, then we obtained the following important SWM backwards results:

1) *Local forcing dominates the Arctic region bias.* Solutions in Arctic region are unchanged whether forcing was allowed or zeroed out south of 30N. (This is useful to eliminate considering the large forcing and bias over the Himalayas.) The bias and forcing were successfully partitioned geographically: various portions of the bias field (e.g. the Beaufort negative bias) can be (and were) successfully isolated from other parts of the bias field.
2) *Some bias regions are independent, some regions are coordinated.* The Barents SLP bias (positive) is linked to the North Atlantic bias (negative) while the Beaufort bias (negative) is not to the North Pacific, Barents, or Atlantic in any strong way.
3) *The North Atlantic/Barents dipole bias and forcing have mixed vertical structure.* The bias field is baroclinic for temperature (T) and equivalent barotropic for vorticity. The associated forcing is: baroclinic T forcing and equivalent barotropic vorticity forcing. For T the largest forcing tends to be at the surface and in the upper model levels. For vorticity the largest values tended to be in the middle or upper troposphere. See figs. 3-1 and 3-2.
4) *The Beaufort region bias and forcing have mixed vertical structure.* The Beaufort region bias is mainly in the stratosphere and warm for T and equivalent barotropic (positive) for vorticity. The associated forcing is equivalent barotropic for T and baroclinic for vorticity; both forcing fields have larger values in the upper troposphere. See figs. 3-3 and 3-4.
5) *Thus the forcing is very different for these two regions of the Arctic bias field.*

B. We used the SWM to see the response of isolated forcing by individual fields.
1) *Artificial thermal forcing could reproduce parts of the SLP bias.* Inspection of the low level T bias field suggests multiple monopoles in T forcing tendency. Elliptically-shaped monopoles of various vertical structures were tested. When a limited number of those T forcing centers are used to force the SWM, one obtains a solution field similar to the SLP bias over the Arctic. See Fig. 3-5.
2) *Specific monopoles seem linked to specific parts of the bias.* A subset of T tendency monopoles (mainly N. Siberia >0 tendency, and Sahara-Arabia deserts <0 T tendency) appear to be the main forcing for Beaufort high <0 bias and Barents >0 bias.

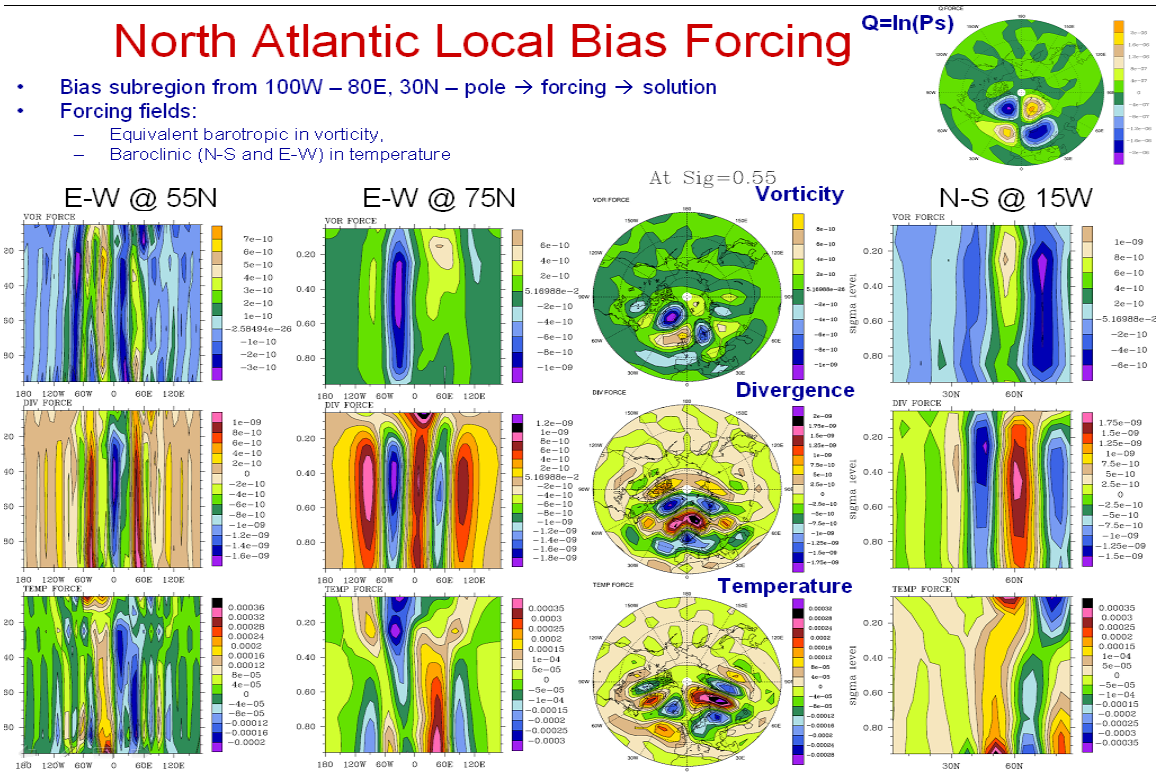

Fig. 3-1: Vertical and horizontal structure of forcing in SWM for North Atlantic & Barents region bias.

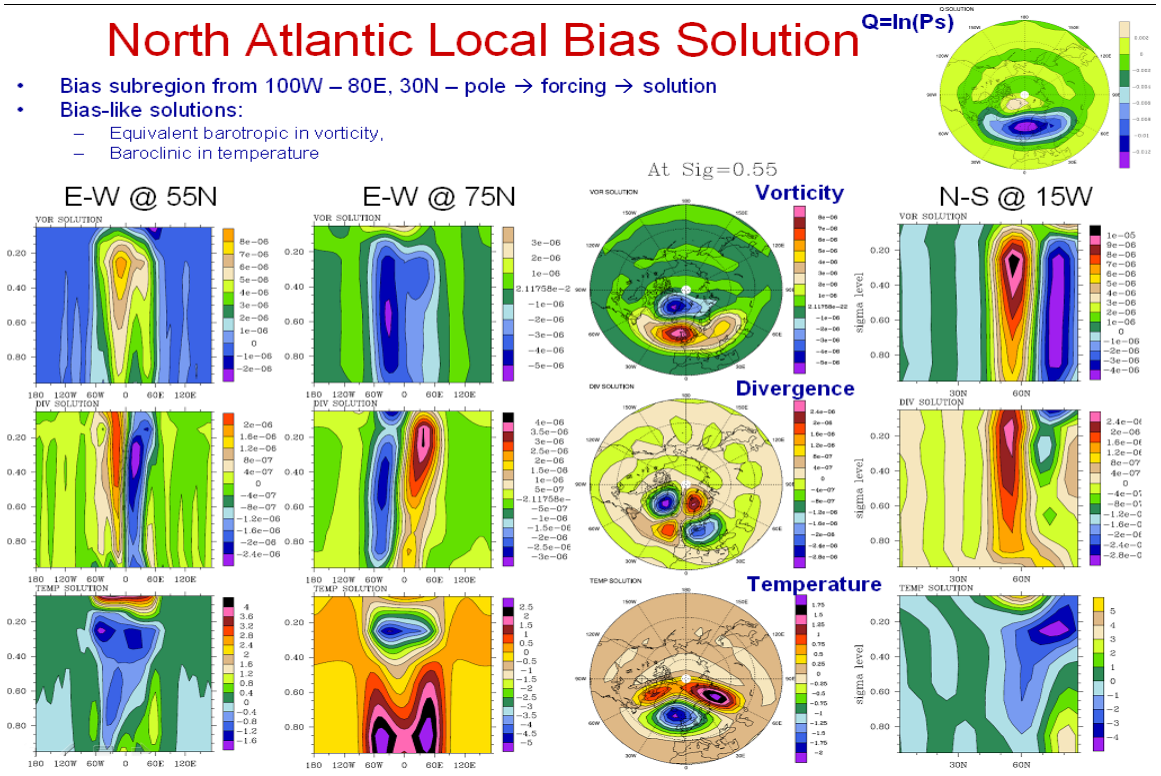

Fig. 3-2: Vertical and horizontal structure of SWM solution created by forcing in figure 3-1.

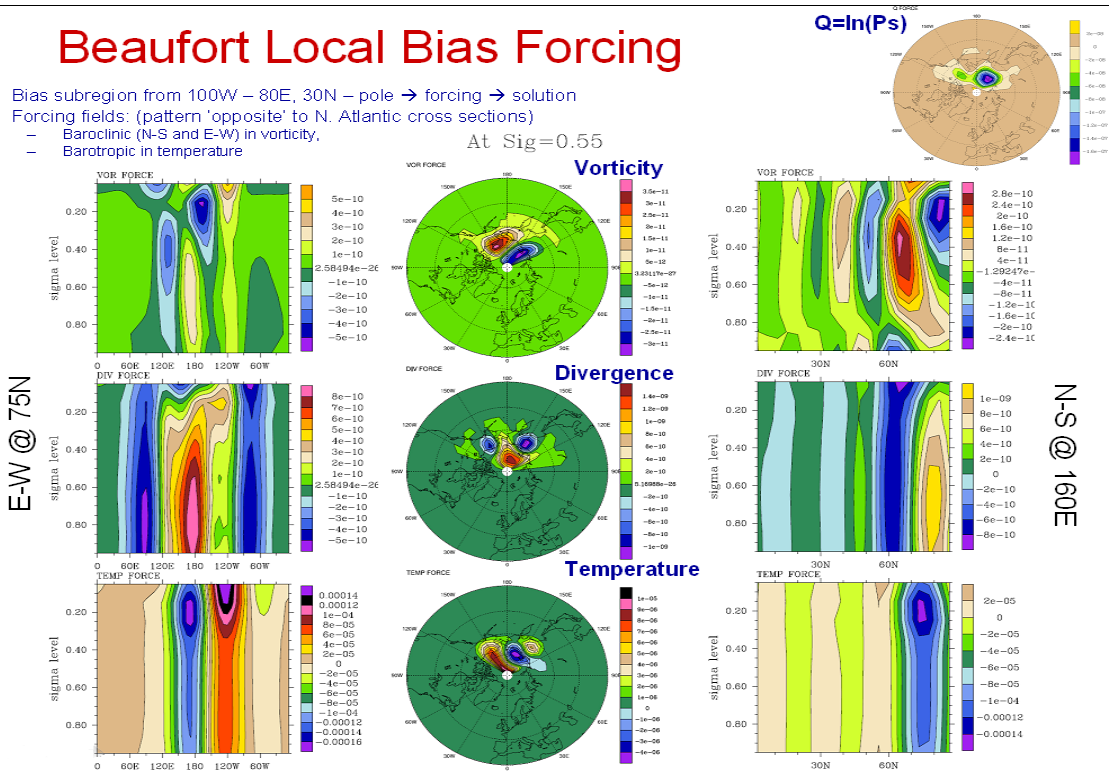

Fig. 3-3. Vertical and horizontal structure of forcing in SWM for Beaufort Sea region bias.

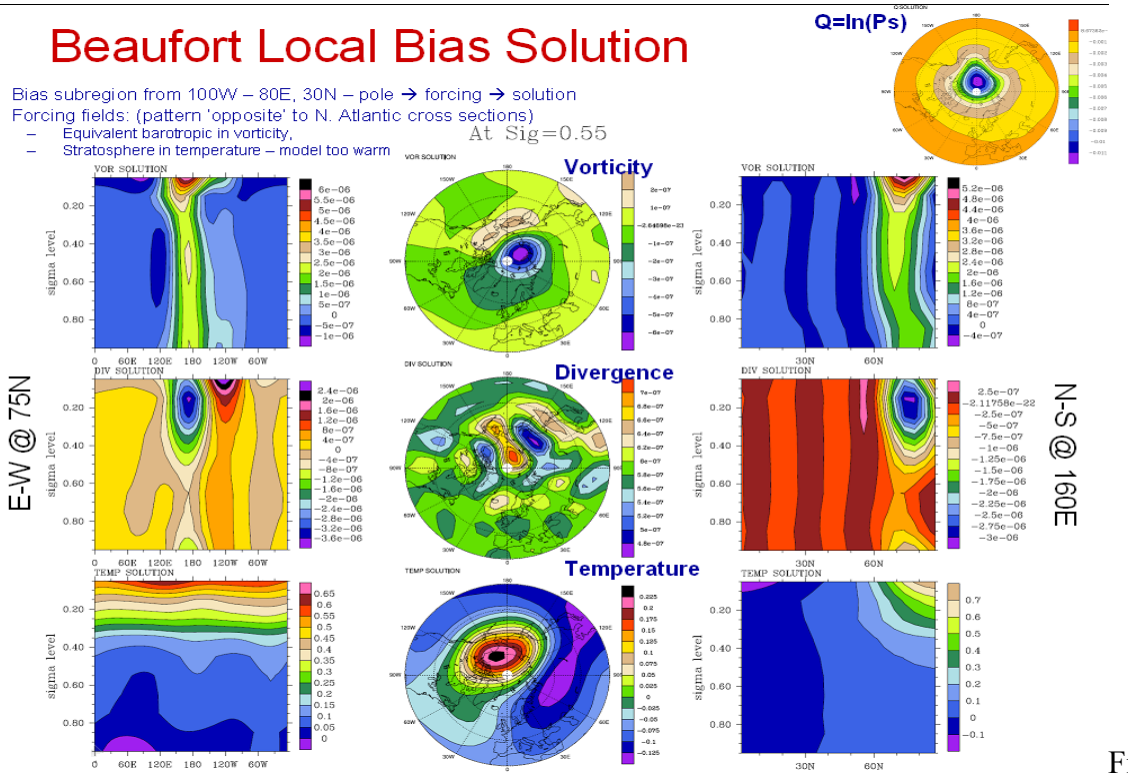

Fig. 3-4: Vertical and horizontal structure of SWM solution created by forcing in figure 3-3.

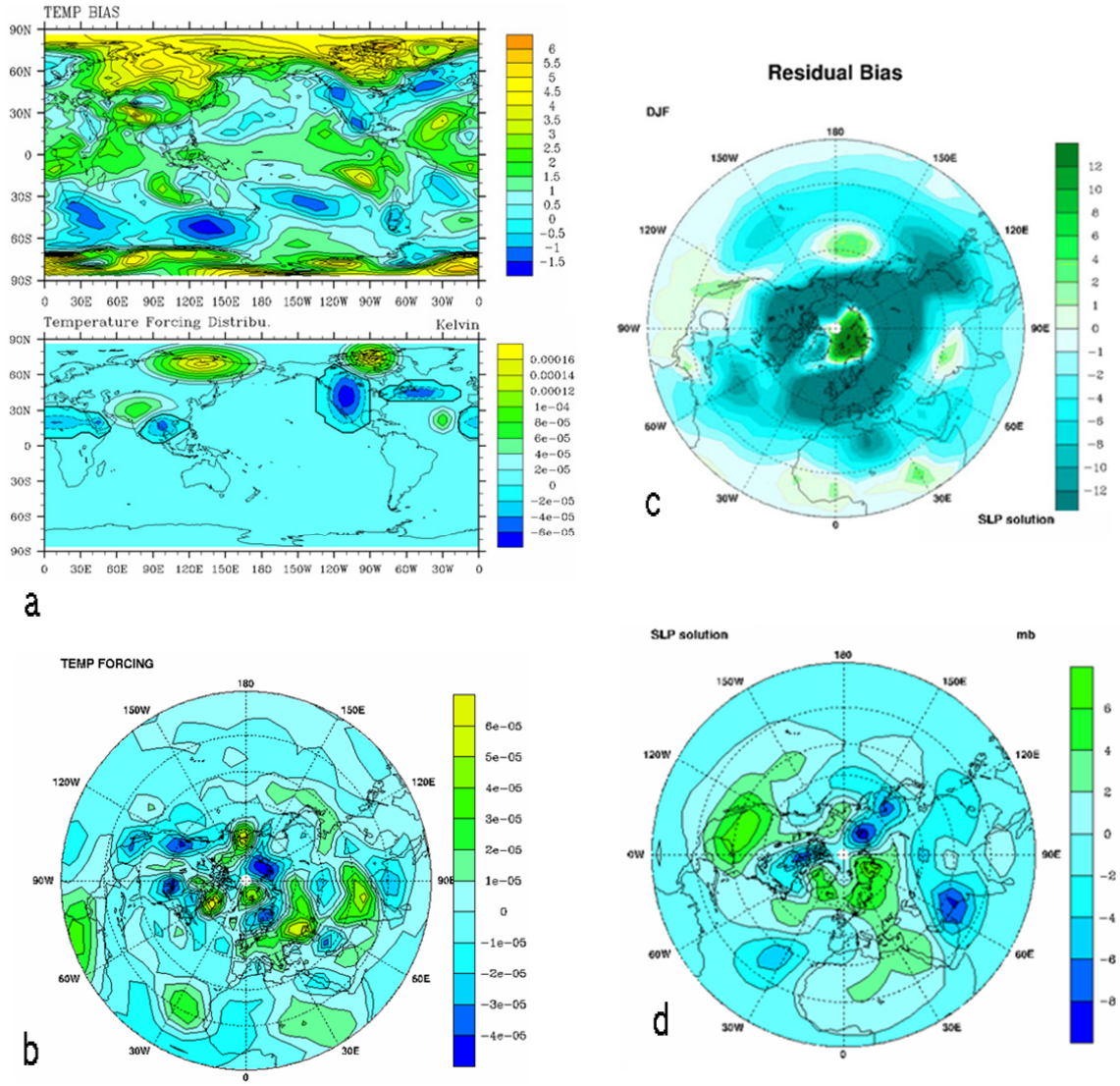

Fig. 3-5. SWM solutions for function-specified monopole temperature forcing. a) Temperature (T) bias at $\sigma = 0.991$ and 9 monopoles of temperature forcing inspired by that T bias. b) Actual temperature forcing from bias field. c) Actual SLP (residual) bias after subtracting the dominant EOF of the CAM model. d) SLP solution from the 9 monopoles in T forcing. Notice how the SLP solution captures most features of the residual bias.

III. April 2007 – March 2008 (Year 4)
In the past 12 months (April 2007 – March 2008) we can report the following activities:

A. We made additional calculations of the solutions obtained from parts of the forcing fields, where the latter are found from running Branstator's SWM 'backwards'. To run the SWM 'backwards' we specify x and find the F. By specifying the bias fields as x, then we obtained the following important SWM backwards results:

1) *Bias solutions from just temperature, just vorticity, just sea level pressure and various combinations of these.* Solutions in Arctic region are predominantly from the temperature and vorticity forcing. Sea level pressure (SLP) also affected by SLP forcing.

B. We formulated and tested a temperature bias equation. This equation is constructed from taking the difference between model and observations for each term of the temperature conservation equation. When evaluated over a long time average (multi-years of the same season) the terms in the temperature bias equation fall into 4 groups of terms:

1. the linear terms in the 'backwards' form of the SWM.
2. the nonlinear terms having bias multiplying bias.
3. the nonlinear terms from time mean contributions from transients.
4. the diabatic heating bias.

Each group of terms may be compared with the forcing found from running the SWM backwards.

1) *Terms 1 (those present in the SWM) are the largest in magnitude in the Arctic region.* This key result validates using the SWM for the study of the temperature bias. This group has largest values in the tropical convective regions (not a focus of this study).

2) *Terms 2 (bias-bias nonlinear terms) are the smallest of the 4 groups of terms.* There is little interaction between the bias and itself. The wind bias has little advection of the temperature bias. This is also an important validation of using the SWM.

3) *Terms 3 (nonlinear transient bias) are horizontal and vertical heat fluxes in ERA-40 data minus the corresponding heat fluxes in the CAM model.* These terms have important contribution mainly in the midlatitude storm tracks, especially the North Atlantic. This is consistent with our working conclusion that mishandling of the North Atlantic frontal cyclones is important for the bias in the 'European side' of the Arctic. The forcing was generally positive across the North Atlantic with some tendency to be larger in the lower troposphere. At low resolutions comparable to the SWM, the pattern tends to be dipolar (positive over Scandinavia, negative over Iberia) consistent with CAM's storm track error.

4) *Terms 4 (diabatic heating bias: CAM minus ERA-40) are found as a residual of a potential temperature conservation equation.* Therefore these terms have slightly different origin than the temperature bias equation, though they are nearly as large as the Terms 1 group. Accordingly, these terms look like the term 1 group in the tropics (a region outside the scope of this study). At the start of the north Pacific and Atlantic storm tracks the term tends to be negative and positive downstream (especially N. Atlantic).

5) *The calculation can be made at much higher (vertical and horizontal) resolution than is possible with the SWM*. However the patterns do change notably between SWM low resolution and much higher CAM resolution. The difference lowered the effectiveness of the forcing found from the SWM to stimulate (or neutralize, depending on the forcing sign) the bias in CAM.

6) *We calculated vertical average heating using precipitation (P) minus evaporation (E) in CAM and ERA-40.* This calculation was suggested by K. Trenberth, who finds the P-E to be acceptably accurate in ERA-40. Results currently under analysis.

C. We made an initial test of the temperature and vorticity forcing fields from the SWM in CAM3.0. The forcing fields were scaled up to T42, 26L resolution. There are large differences in how friction and diffusion are handled in the SWM versus CAM; one difference concerns the high wavenumber dependence in CAM that cannot be used in the SWM. Various tests were tried. The response of CAM to the added forcing has some elements of the bias (a successful result) however, additional tests are needed.

D. Our plans for the next grant extension. We shall finish our analysis of the temperature bias equation. We shall formulate and study results from a vorticity bias equation. We intend to make a few more test runs of CAM with appropriate forcing.

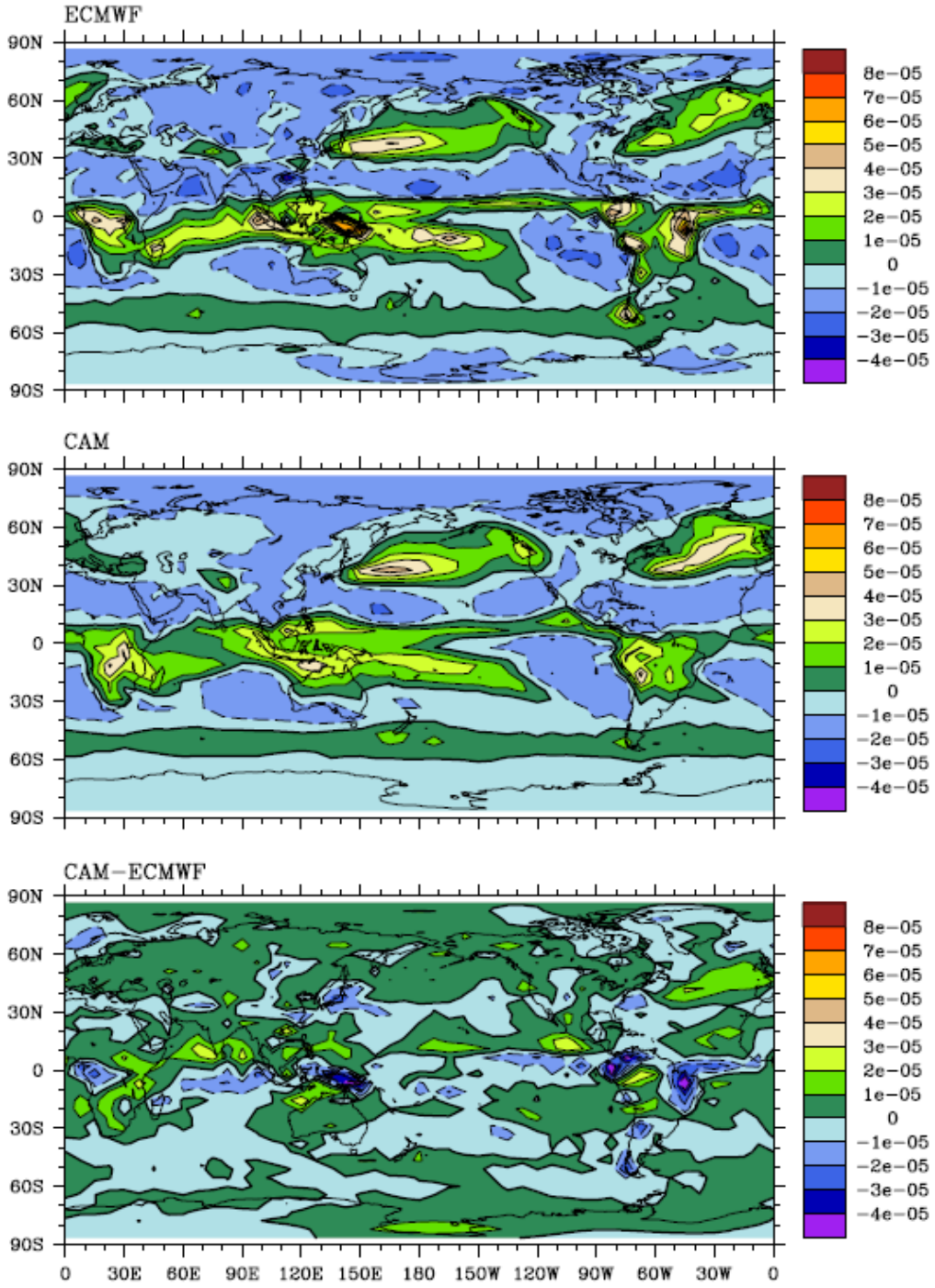

Fig. 4.1. Diabatic heating during DJF. Top panel uses ERA-40 data; middle panel in CAM3.0 T42 AMIP simulations; bottom panel is difference field: CAM minus ERA-40. The bottom panel is the same as terms 4 in the temperature bias equation. Level is sigma =0.7.

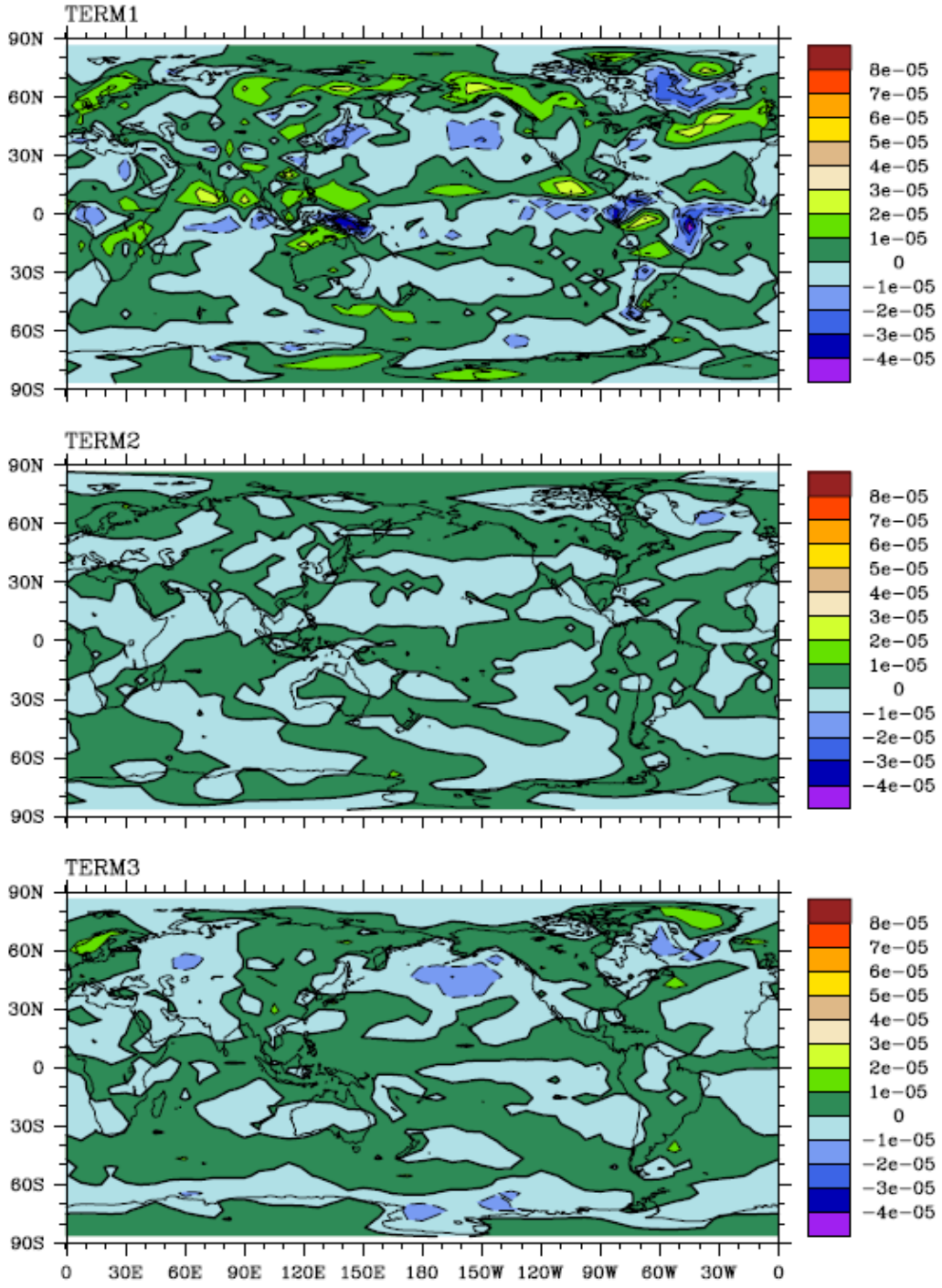

Fig. 4.2. Groups of terms in the temperature bias equation. Term1 are all terms in the SWM. Term2 are all nonlinear bias-bias terms. Term3 are transient terms. The level is sigma=0.7.

IV. April 2008 – March 2009 (Year 5)
In the past 12 months (April 2008 – March 2009) we can report the following activities:

A. We made additional calculations in support of the temperature bias equation (TBE) and the vorticity bias equation (VBE) papers to be published in Climate Dynamics (CD).

1. The TBE is the difference between the temperature equation as seen in the CAM3 model data minus the corresponding equation in the ERA-40 data. All terms are time averaged. This is a 'primitive equation' for the time mean temperature bias. The diabatic heating term was evaluated several ways (as a consistency and accuracy check) for evaluating it as a residual. Terms were grouped into logical sets: linear (in the bias) terms (mainly advection); nonlinear (in the bias) terms; time mean contributions from transients (mainly heat fluxes); and diabatic processes. Geographic (3-D) distributions of these groups were examined.
2. The VBE is obtained in a similar manner as was the TBE. Terms are grouped into the same types of categories: linear, nonlinear, transients, diabatic (friction and diffusion).

B. The TBE paper was submitted to CD (and accepted in early June, 2009)

1. Nonlinear terms small except for ICZ and some midlatitude surface locations (needed to use the SWM in CD paper 3)
2. Diabatic and Linear advection terms are the largest
3.-8. Several conclusions were drawn about the north Atlantic storm track (NAST): Linear advection terms dipolar pattern (due to storm track shift, negative NW of positive). The transient advection terms are larger in upper troposphere and postitive. The diabatic heating bias is large, mainly from precipitation, secondly by vertically averaged net radiation. The downstream end of the NAST is shifted too far south (~10-15 degrees latitude)This shift of NAST creates a SLP bias that autocorrelates with Barents Sea area SLP bias; the SWM links Arctic bias to local and NAST region forcing.
9. North Pacific storm track (NPST): Transient terms >0 upper troposphere, <0 mid & lower troposphere
10. Diabatic heating large in tropics, CAM3 emphasizes NH ICZ

C. In addition, some specific things were uncovered about the vertically integrated heating that were also included in the TBE paper:

1. Q1=R+SHF+L*P bias is dominated by heating bias (>0) over the north Atlantic, north Pacific, North American W. coast
2. Net radiative cooling (=R) at top of atmosphere (TOA) shows cooling bias over Arctic Ocean,
3. Over NAST & Russia Q1>0 mainly from Precipitation (P), also R.
4. In the NPST: surface sensible heat flux (SHF) too weak at start (<0)-- opposite to the NAST; while P & R biases >0 at end.

-
The Climate Dynamics (CD) paper on the temperature bias equation (TBE) is the first of 3 that form the backbone of the research project. The remaining 2 papers are being written and

should be submitted before the final report is filed. The TBE paper has these major conclusions:

-

The final report will list conclusions for the other two CD papers currently in preparation: VBE, and other results (mainly results from the SWM studies). Some vorticity related results are included here as figures 5.4 and 5.5.

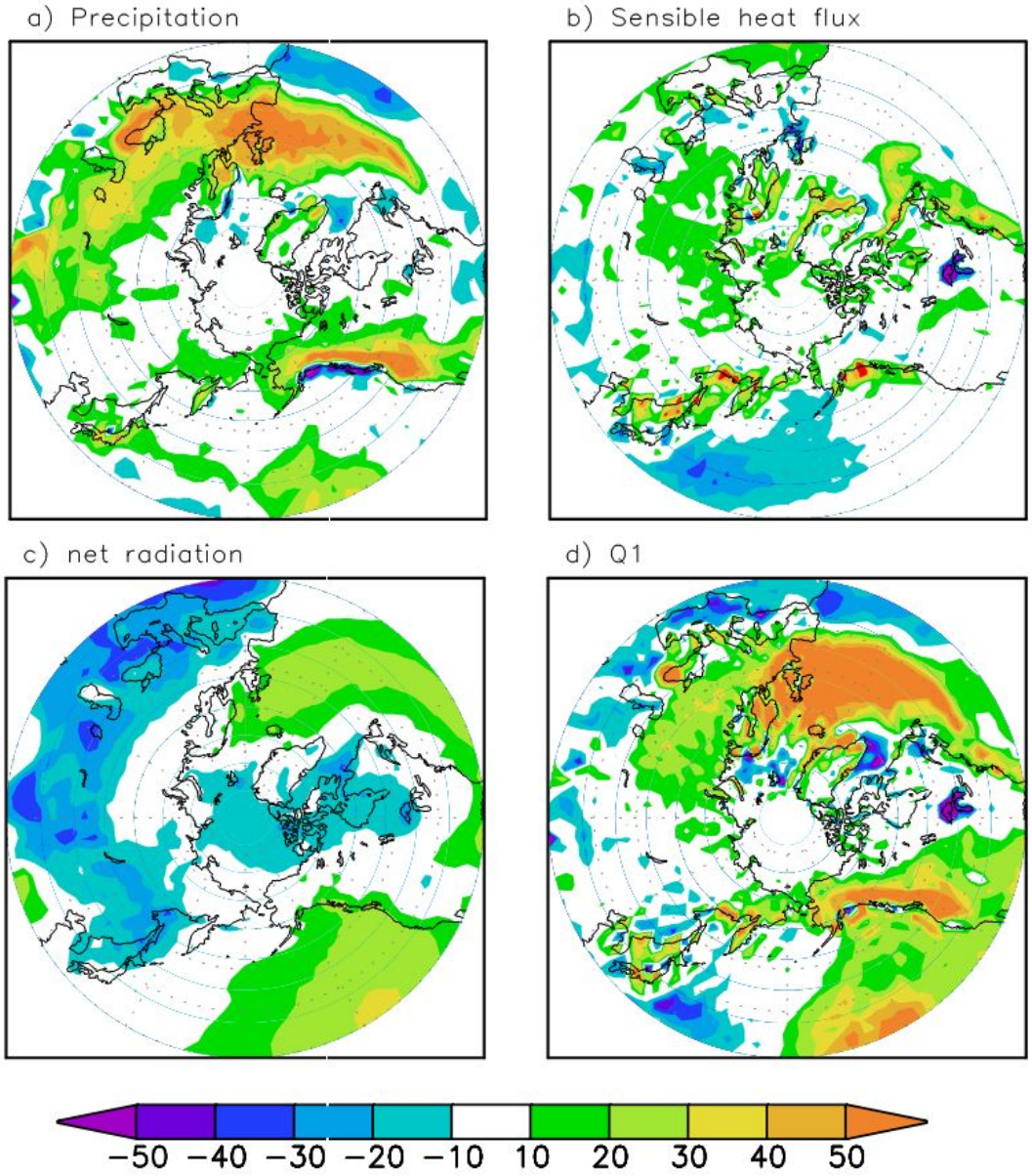

Fig. 5.1 Vertically integrated heating bias components. a) vertically integrated latent heating (L*P) bias. b) Surface sensible heat flux bias. c) Top of atmosphere net radiation bias. d) Total heating, Q1. The Q1 bias for the NAST is mainly from excessive precipitation in the model. It may be related to the storm track being too far south in the model (tapping subtropical moisture) but that conclusion is at best a partial explanation since there is no corresponding negative bias on the north end of the NAST. Associated with that is P bias is less cooling in the model. Sensible heat flux bias differs for the NAST and NPST causing storms to start differently in the two tracks.

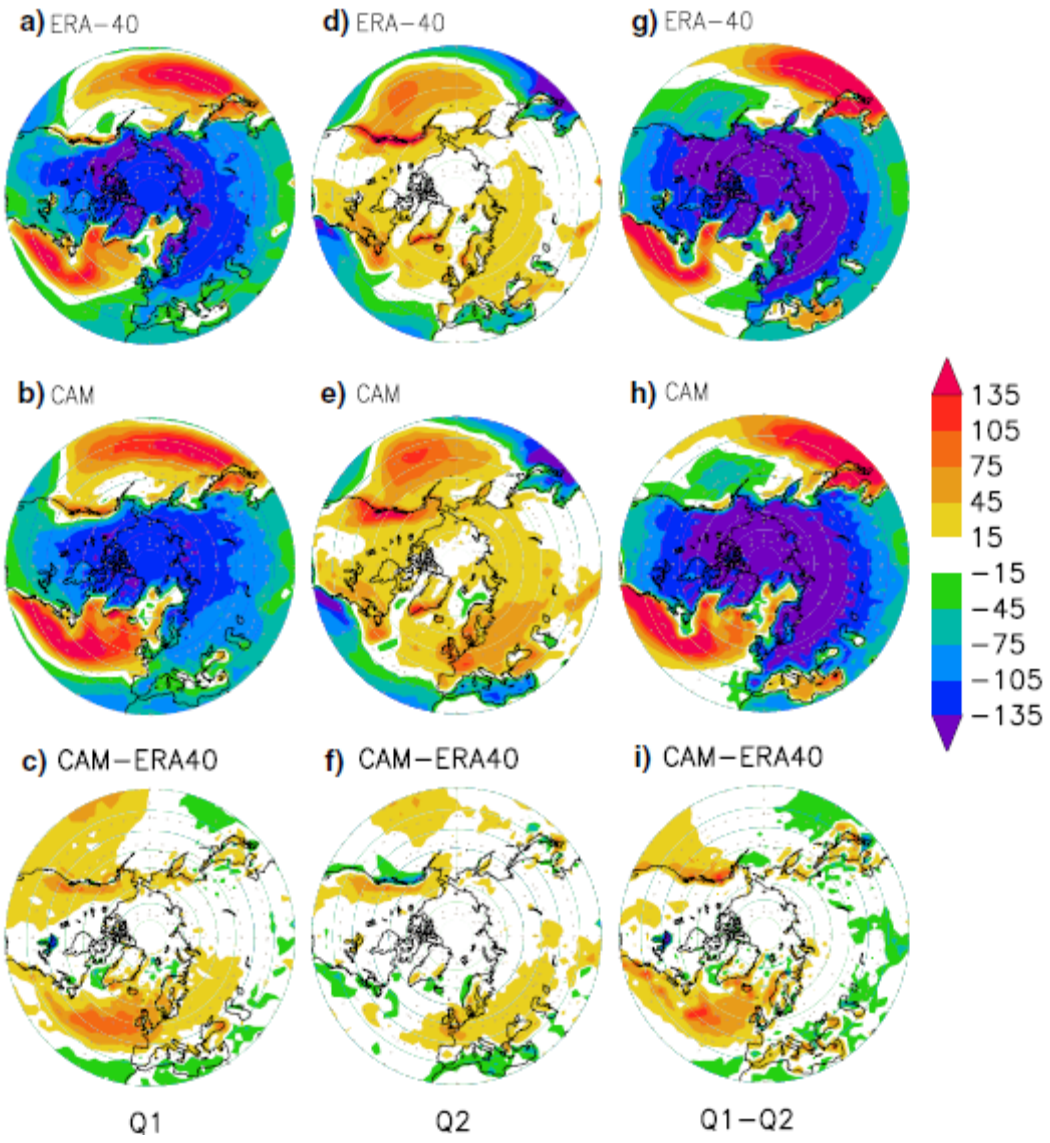

Fig. 5.2 Implied heating from the moisture equation (middle), Q2 = L*(P-E). Total energy equation heating (right) Q1-Q2. Vertically integrated diabatic heating in a ERA-40 and b CAM3 data and their bias c for latitudes north of 30_N, otherwise comparable to d–f. Plot c, same as d, is shown here for reference. Middle column d–f are corresponding quantities of vertically integrated boundary moisture contribution expressed as heating [latent heat times (precipitation minus evaporation)]. g–i are corresponding quantities for a total energy equation. Units are W m^{-2} . The NCEP/DOE AMIP reanalysis II data also have stronger sensible (and latent) heat fluxes over the Gulf Stream, but CAM3 data amplify that difference even more so reanalysis data differences probably cannot account for this bias. In summary for the NAST, CAM3 has greater sensible heat flux at the start, greater evaporation and precipitation along the entire NAST (even beyond into western Asia, were negative net radiation is also stronger). While these processes are stronger in CAM3, the transient heat flux (fig. 5.3) is weaker as are other measures of the storm track strength (fig 5.4)!

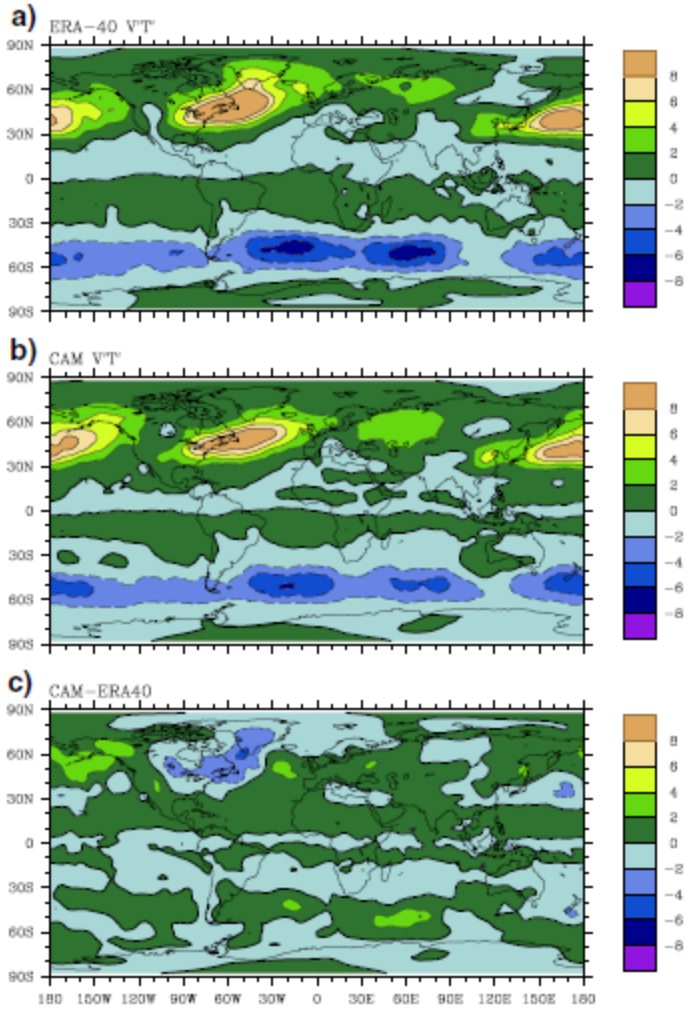

Fig. 5.3. Band passed (2-8 days) northward heat flux per unit mass during DJF at σ=-.5 in a) ERA-40, and b) CAM3 data. The bias is in c). Dashed contours used for southward flux. This measure of frontal cyclone storm strength and track emphasizes the early stages of the cyclones. CAM3 track is narrower, and centered further south than ERA-40 data. However, the magnitude is generally weaker, so a dipolar track error is less prominent than the narrower, weaker cyclones by this measure.

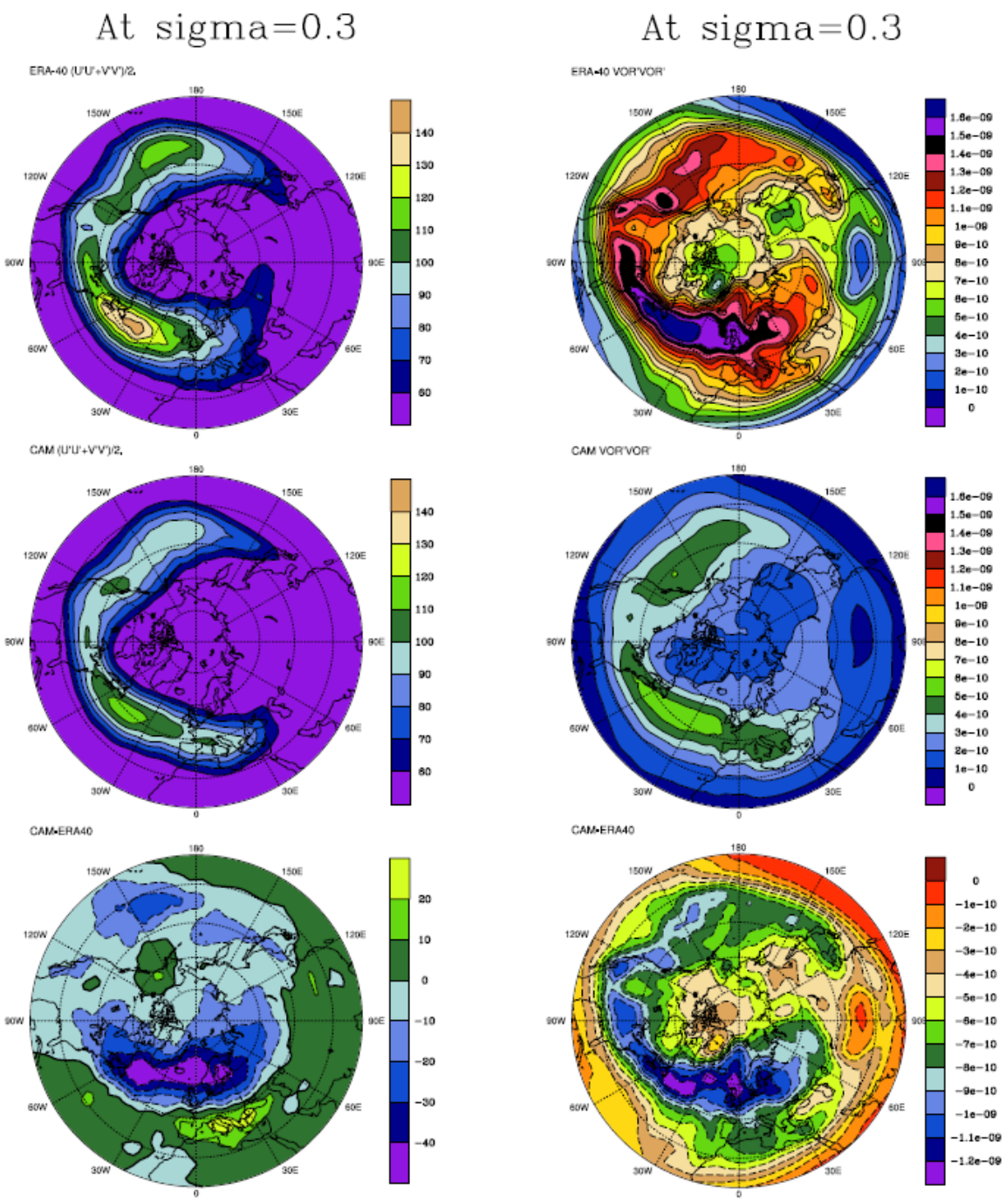

Fig. 5.4, Left column: band passed (2-8 day) transient kinetic energy KE' for ERA-40, CAM, and bias. Right column: band passed enstrophy, Ens' for ERA-40, CAM, and bias. These quantities both emphasize the downstream end of the storm tracks. The KE' is uniformly ¼ to 1/3 smaller in CAM3. The Ens' is uniformly 2 to 3 times larger in ERA-40. One might think this is due to the higher wavenumbers kept by the model used to create the ERA-40 data, but in fact nearly all the wavenumbers have less amplitude in CAM3, including planetary waves.

Table 1. Vorticity Equation Terms Ranking

DJF, Northern Hemisphere Middle and High Latitudes♪

Level	σ = 0.3			σ = 0.7		
Data	ERA-40	CAM3	Bias	ERA-40	CAM3	Bias
$v\frac{\partial\zeta}{\partial y}$	1	1	1	2*	5*	3*
$u\frac{\partial\zeta}{\partial x}$	2	2	2	4	5*	3*
$f\frac{\partial\omega}{\partial p}$	3	3	4	5*	1*	3*
βv	4	4	5	2*	1*	6
Fr	5	5	3	5*	3*	1*
$\zeta\frac{\partial\omega}{\partial p}$	6	6	6	8	9	9
$\omega\frac{\partial\zeta}{\partial p}$	7	7	8	1	3*	1*
$\frac{\partial\omega}{\partial x}\frac{\partial v}{\partial p}$	8	8	7	7	5*	8
$\frac{\partial\omega}{\partial y}\frac{\partial u}{\partial p}$	9	9	9	9	5*	7

♪ Areas of steep or high topography, such as near Greenland excepted

* peak magnitudes over substantial area are essentially the same

Fig. 5.5. Ranking of vorticity equation terms. While upper troposphere rankings are similar, CAM3 has quite different behavior in the lower troposphere; in particular friction is much stronger in CAM3.

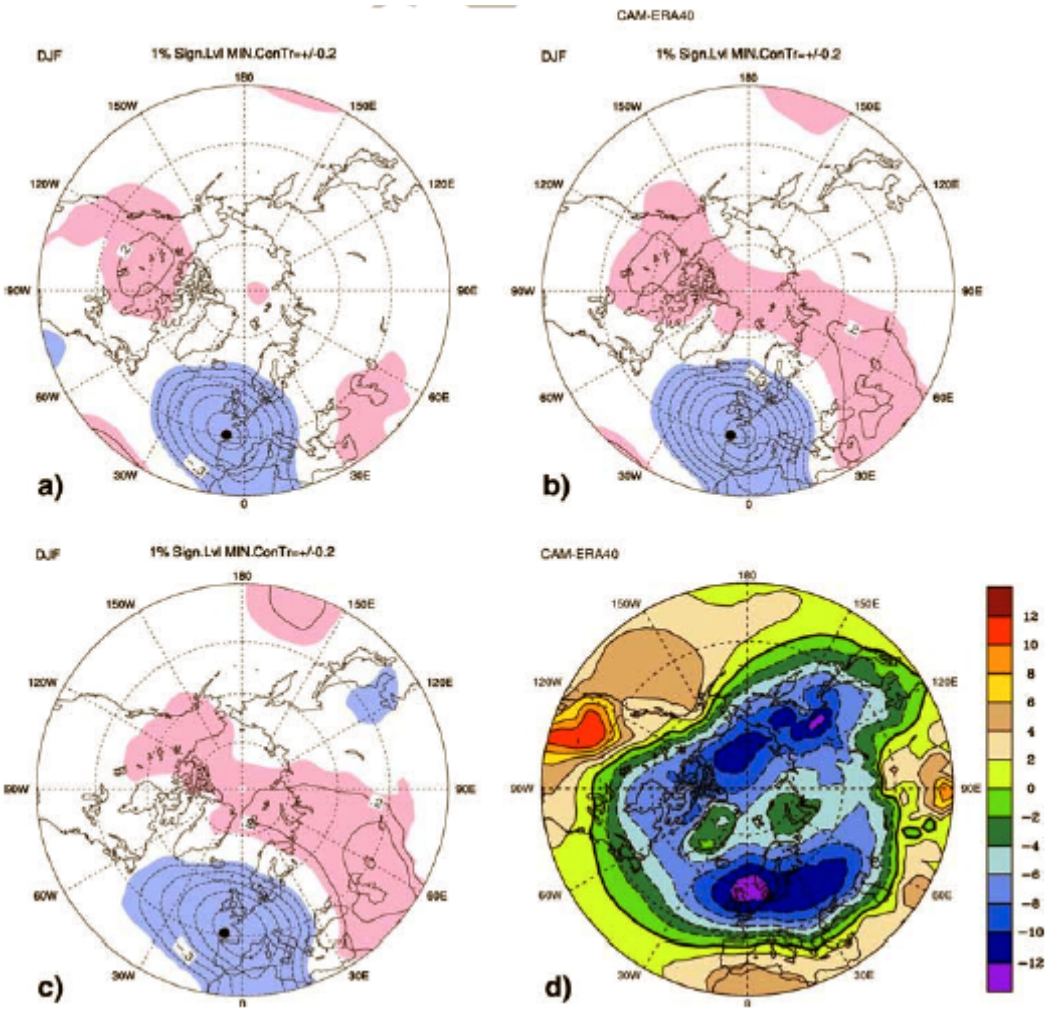

Fig. 5.6. One-point correlations between P at 7.5W, 45N and sea level pressure (SLP) at various lags. All data from DJF months of a 20 year CAM3 AMIP simulation and low pass (>10 days) filtered. Shaded areas are significant at the 1% level. -0.1, 0, 0.1 contours suppressed. a) SLP leading P by 3 days, b) no lag, c) SLP following P by 3 days. Higher SLP over the Barents Sea follows more P (and lower SLP) near Iberia. d) This SLP combination is also seen in CAM3's SLP bias. This and other evidence from SWM calculations supports the conclusion that the model's error in handling the downstream end of the NAST is linked to the surface climate bias on the 'European side' of the Arctic.